Bull. Inst. Chem. Res., Kyoto Univ., Vol. 69, No. 2, 1991.

Epitaxial Growth of Lead Chalcogenides on Tin Telluride (001)

Shinsuke FUJIWARA*, Masahiro TSUJI*, Yoshikazu FUJII*, Yasufumi SUSUKI*, Kenji KIMURA* and Michi-hiko MANNAMI*

Recieved June 4, 1991

Process of epitaxial growth and interfacial structures of PbS, PbSe and PbTe on SnTe (001) surface are studied by transmission electron microscopy, electron diffraction and scattering of MeV He ions. Structure and distribution of misfit dislocations at the interfaces are clarified.

KEY WORDS: Epitaxy/Narrow-gap semiconductors/PbS/PbSe/PbTe/SnTe

INTRODUCTION

Lead chalcogenides are typical narrow gap semiconductors having NaCl-type crystal structure. Good single crystals of these materials can be prepared by vacuum epitaxial growth on the {001} surface of some alkali halides.[1,2] Growth of PbSe on PbS(001) has been extensitvely studied with TEM (transmission electron microscopy) in relation to the formation of misfit doslocations at the interface of the crystals, and the results were reviewd by Mathews[3] and Honjo and Yagi[4]. The PbSe crystal grows on PbS by layer-by-layer process. The misfit dislocations are introduced on the interface of the two crystals during the growth, and are edge type parallel to the ⟨110⟩ on the (001) interface.

On the other hand, it is known that tin telluride (SnTe), having NaCl-type crystal structure, shows good epitaxial growth on the {001} surfaces of NaCl and KCl single crystals. We use the SnTe grown on the KCl(001) as the substrate crystal for the epitaxial growth of lead chalcogenides, as it is expected that the so called "layer-by-layer" growth of the chalcogenides takes place.

We have been studying ion-surface interaction processes with the use of the clean (001) surfaces of epitaxial lead chalcogenides and tin telluride single crystals simply because these crystals yield good flat surfaces by epitaxial growth under UHV conditions.[5] In the present paper, we summarise our studies of the epitaxial growth of lead chalcogenides on the {001} surface of SnTe, which we could not report in our papers on the ion-surface interaction studies. For the characterisation of the surfaces we used TEM (Transmission Electron Microscopy), RHEED (Reflection High Energy Electron Diffraction), RBS(Rutherford backscattering)/ channelling of MeV He ions and MeV ion scattering at glancing angle incidence on the crystal surface under UHV (Ultra High Vacuum) conditions. Process of epitaxial growth, and structure of surfaces and interfaces are studied.

* 藤原 伸介, 辻 雅裕, 藤居 義和, 鈴木 康文, 木村 健二, 万波 通彦: Department of Engineering Science, Kyoto University, Kyoto 606-01

EXPERIMENTAL

Single crystal of SnTe was grown on the cleavage {001} surface of KCl kept at 200°C by evaporation of pure SnTe (purity 99.999%) under a pressure of the 10^{-6} Torr range. The SnTe crystal was more than 30 nm thick. Pure lead chalcogenides (PbS, PbSe and PbTe) were then evaporated on the {001} surface of the SnTe crystal at the same temperature. Thickness of the evaporated materials was measured with a quartz oscillator microbalance. For the TEM observation of the crystals, the substrate KCl was dissolved into water and the crystals were observed under an electron microscope (Hitachi, HU11). RBS/channelling of MeV He ions from the crystals thus prepared was done with a beam of MeV He ions from the 4 MV Van de Graaff accelerator of Kyoto University.

RHEED and ion scattering studies of epitaxial crystals with clean surfaces were performed under UHV conditions. Freshly cleaved KCl single crystal was mounted in a 5-axis goniometer in a UHV chamber and the growth of SnTe was done under a pressure of 10^{-9} Torr. Lead chalcogenide was then evaporated on the surface of SnTe kept at 200°C. During and after the growth of the crystals, their surfaces were observed with 20 keV RHEED. The UHV chamber was connected to 4 MV Van de Graaff accelerator of Kyoto University via a differentially pumped section. The crystals on the goniometer under the vacuum of the 10^{-9} Torr range were irradiated by a beam of momentum-analysed ions from the accelerator. Backscattered ions or ions scattered at small angles at glancing angle incidence of the ions on the surface of the crystal mounted in the goniometer were detected by solid state detectors.

RESULTS AND DISCUSSION

1. SnTe/KCl

At the very initial state of growth of the SnTe, many well-defined islands are formed, where the SnTe islands are in the orientation relationship,

$$SnTe_{(001)}//KCl_{(001)}$$
$$SnTe_{[100]}//KCl_{[100]}.$$

The interface between SnTe and the substrate KCl could not be observed. The islands are collapsed into a continuous single crystal foil at mean thickness about 20 nm. From the distribution of dislocations as shown in Fig. 1, where the growth was done at lower substrate temperature, it is supposed that the dislocations are introduced in between the islands of SnTe during the coalescence of the islands. The SnTe crystals thus prepared are free from defect other than the dislocations. The {001} surface of the SnTe crystal observed by RHEED under UHV conditions is shown in Fig. 2, and it was concluded from these diffraction patterns that no reconstruction occurs on the surface and that the (001) surface has bulk exposed structure. This was confirmed by RBS/channelling study of the surface by MeV He ions.[8]

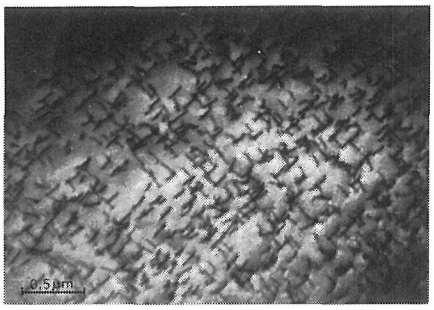

Fig. 1 Dislocations in SnTe crystal of 630 nm thick (by Y. Kawagoe.[6])

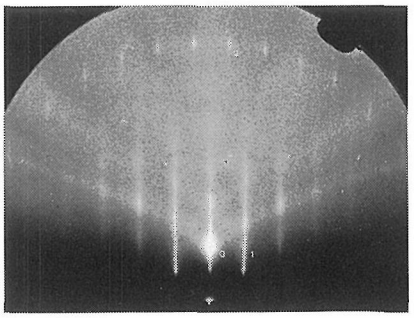

Fig. 2 Reflection high energy electron diffraction pattern from a clean (001) surface of SnTe. 20 keV electrons. (by H. Kawauchi[7])

2. PbSe/SnTe

TEM observation and RBS/channelling study[8] of the PbSe/SnTe bicrystals showed that no island of PbSe is formed on the SnTe surface during the growth of PbSe. This suggests that the mode of growth of PbSe on the (001) surface of SnTe is "layer-by-layer" process. Misfit dislocations are introduced on the (001) interface when the overlayer PbSe crystal is more than 1 nm thick. An example of the misfit dislocations is shown in Fig. 3, where a cross-network of misfit dislocations are seen. The dislocations are edge-type and are parallel to the [110] and [1$\bar{1}$0] directions on the (001) interface. Density of the dislocations depends on the thickness of PbSe and the dependence of the density on the thickness of PbSe is shown in Fig. 4. The density becomes a constant at thick PbSe layers, which is almost equal to that calculated from the lattice constants of the two crystals. RHEED and RBS/channelling study of the (001) surface of PbSe showed that the (001) surface of PbSe has bulk exposed structure, and that the PbSe is pseudomorphic to the substrate SnbTe at the thickness less than

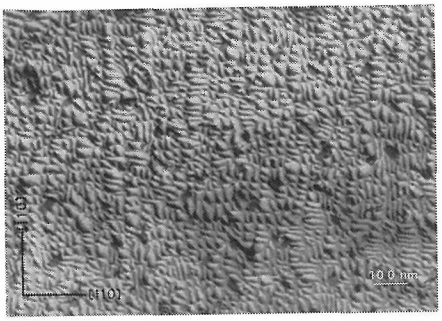

Fig. 3 A network of misfit dislocations on the (001) interface of a PbSe/SnTe bicrystal, where the thicknesses of the overgrown PbSe and substrate SnTe are 2 nm and 60 nm respectively.

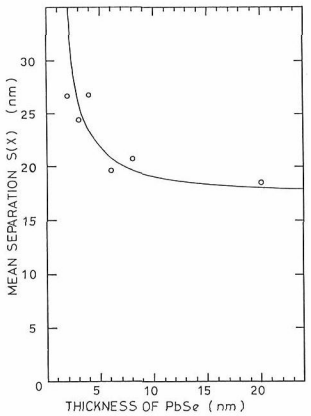

Fig. 4 Dependence of the density of misfit dislocations in PbSe/SnTe bicrystal on the thickness of PbSe.

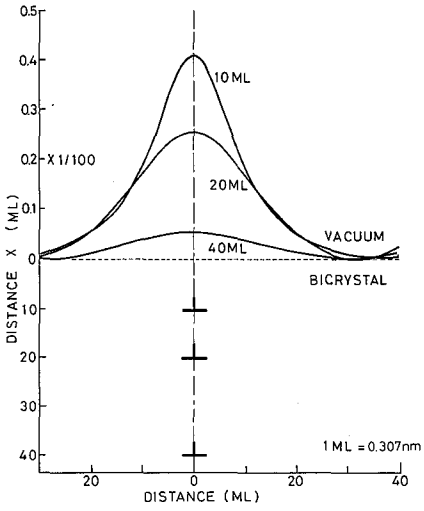

Fig. 5 The distorted (001) surfaces of PbSe/SnTe bicrystals with misfit dislocations parallel to the surface. The edge dislocations with Burgers vector parallel to the surface are at 10 ML, 20 ML and 40 ML from the surface (1 ML = 0.3 nm).

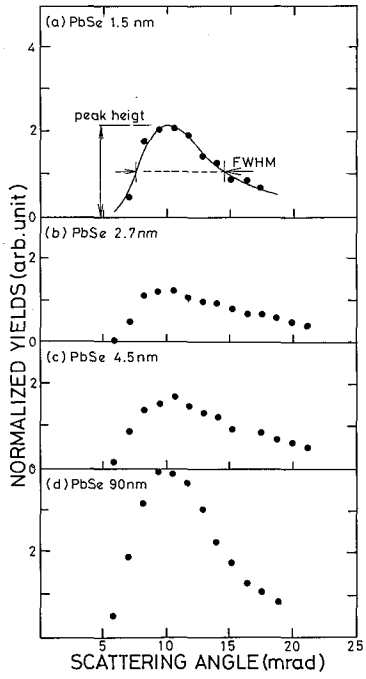

Fig. 6 Examples of the angular distributions of He ions scattered at small angles at glancing angle incidence of 0.7 MeV he ions on PbSe/SnTe surface. The distribution becomes broader with increasing thickness of PbSe and then recovers at PbSe thicknesses about 30 nm.

about 3 monolayers.[8]

Now suppose an edge dislocation with Burgers vector parallel to a surface is on a plane parallel to the surface. The surface must be distorted when the distance of the dislocation from the surface is small, as the surface is strained by the elastic field of the dislocation. From the elastic theory of dislocation developed by Eshelby,[9] the change in the shape of a flat surface was calculated at the introduction of an edge dislocation near the surface. Fig. 5 shows the calculated surface distortions, where the scale normal to the surface is elongated as shown in the ordinate (1 ML = 0.3 nm). The surface protrudes just above the dislocation and the protrusion is larger for dislocations nearer the surface. The distortion becomes negligibly small for dislocations at 50 nm apart from the surface. In the present PbSe/SnTe bicrystals, the misfit dislocations cannot move away from the interface and the distance of the dislocations from the surface is equal to the thickness of the PbSe layer. It is expected therefore that the surface of PbSe/SnTe is wrinkled by the cross-network of misfit edge dislocations when the PbSe layer is thin.

In order to detect the surface wrinkle of the PbSe/SnTe bicrystal, we studied glancing angle scattering of MeV He ions from the surfaces of PbSe/SnTe bicrystals

during the growth under UHV conditions. At glancing angle incidence of MeV ions on an atomically flat crystal surface, most of the ions are specularly reflected, since the transverse velocities of the ions (in the direction normal to the surface) are smaller to overcome the potential barrier formed by the topmost atomic plane. Thus the ions can penetrate the surface only at surface steps. At larger glancing angle incidences the ions penetrate the surface as the transverse velocities of the ions are large enough to surmount the potential barrier, and thus there is a critical angle for specular reflection. The angle is about 12 mrad for 0.7 MeV He ion at SnTe(001).

An example of a series of measurements of the angular distribution of scattered He ions is shown in Fig. 6 at the incidence of a beam of 0.7 MeV He ions on PbSe/SnTe during the prowth of PbSe. The angle of incidence of the He ions on the surfaces was 5 mrad. The angular distribution from the substrate SnTe surface is peaked at the angle which is twice as large as the angle of incidence. The distribution becomes broader and the ion yield at the angle of specular reflection becomes smaller as the thickness of the PbSe layer increases. The distribution becomes the broadest at PbSe layer of thickness about a few nm, and then becomes sharper again at thicker PbSe layers.

At the present geometry of incidence of the ions on the wrinkled surfaces, the ions are scattered away from the angle of specular reflecton of otherwise flat surface. They also penetrate the surface at some area where the angle of incidence exceeds the critical angle for reflection. The angular distribution of the reflected ions is thus blurred and the yield of ions at the angle of specular reflection becomes smaller. The observed decrease in the yield and broadening of the angular distributions at a few nm thick PbSe are caused by the increase in the surface distortion by newly introduced misfit dislocations. As the surface distortion becomes smaller with the increasing PbSe thickness, although the density of dislocations increases, the angular distribution becomes sharper again.[10] Observed change in the energy spectrum of the specularly reflected ions with the thickness of PbSe film is consistent with the change in the angular distribution, i.e. the fraction of ions penetrated through the surface increases when PbSe is about a few nm thick.

In our previous study of the surfaces of PbSe/SnTe by RBS/Channelling of MeV ions, we found pseudomorphic growth of PbSe on SnTe(001) at PbSe thicknesses less than about 1 nm. We also found that an anomalous increase in the yields of ions scattered from Pb and Te atoms from thin surface layers of PbSe of thicknesses more than about 1 nm. The increases suggested that Pb and Te atoms are displaced from their lattice sites viewed parallel to the surface normal, however, we could not find the origin of such lattice disorders. Now it becomes clear from the glancing angle scattering of He ions that the lattice disorders are caused by lattice distortion around the misfit dislocations.

3. PbS/SnTe and PbTe/SnTe[11]

Orientation relationships of these systems are same as that of PbSe/SnTe. The growth takes place by "layer-by-layer" in both systems. TEM observation showed that the process of growth of PbTe on SnTe(001) is equal to that of PbSe on SnTe(001),i.

e. the misfit dislocations are formed on the interface and the density of the dislocations increases with the increasing thickness of PbTe. An electron micrograph of PbTe/SnTe is shown in Fig. 7(a), where a square network of misfit dislocations is seen on the interface. The final mean separation of dislocations was 32 ± 5 nm and was larger than the separation 21 nm calculated from the lattice constants of the crystals. On the other hand, PbS/SnTe bicrystals showed only moire fringes, and did not show such a network of misfit dislocations. Very rarely irregular dislocations are seen on the interface, an example is shown in Fig. 7(b). Misfit of bicrystals is defined by $f = 2(a_s - a_o)/(a_s + a_o)$, where a_s and a_o are the lattice constants of substrate and film respectively. Misfit of PbS/SnTe is 6.4×10^{-2}, and the mean separation of the misfit dislocations is expected to be 6.8 nm. We could not find the reason for the disappearance of the misfit dislocations in PbS/SnTe system, but perhaps one of the reasons is the larger misfit of PbS/SnTe compared with that of PbTe/SnTe where the misfit is -2.1×10^{-2}.

It was shown that RBS/channelling is useful for the study of interface of bicrystals with larger misfit.[12] In order to confirm this TEM observation, the PbTe/SnTe and PbS/SnTe bicrystals were studied by RBS/channelling of MeV He ions. Energy spectra of He ions backscattered from the target crystals were measured with a solid state detector. The [001] aligned and random spectra of He ions from PbTe/SnTe and PbS/SnTe bicrystals are shown in Fig. 8. He ions scattered from Pb atoms have energies larger than those scattered from Sn, Te, Se and S atoms, and the information of the interfaces must be observed at the lower energy edges of the scattering from Pb atoms. As it is seen from the aligned energy spectrum from PbTe/SnTe, an anomalous increase in the yield of ions is seen as a peak at the lower energy edge from Pb scattering as indicated by shadow. The increase is due to the direct scattering of ions from the dislocations on the interface. No such peak is seen in the aligned spectrum fromn PbS/SnTe, and this shows that there is no dislocations on the PbS and SnTe interface.

It is interesting to note that the formation of misfit dislocations depends on the size of the substrate SnTe. Fig. 9 shows an electron micrograph of PbTe/SnTe, where the substrate SnTe has island structure. The thicknesses of the SnTe islands are less

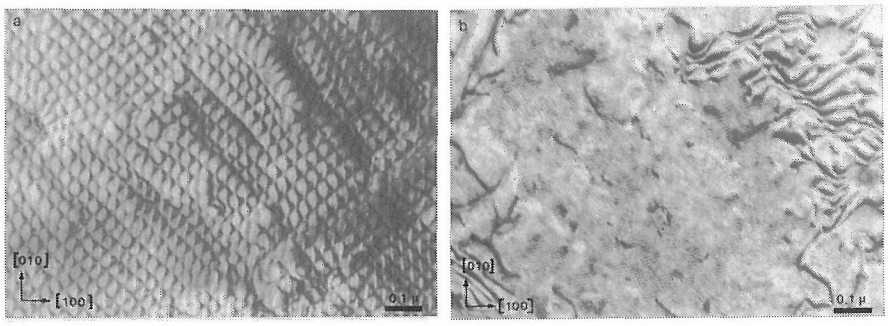

Fig. 7 Transmission electron micrographs of (a) PbTe/SnTe and (b) PbS/SnTe. A regular network of misfit dislocations is seen in (a), while no such network is found in (b).

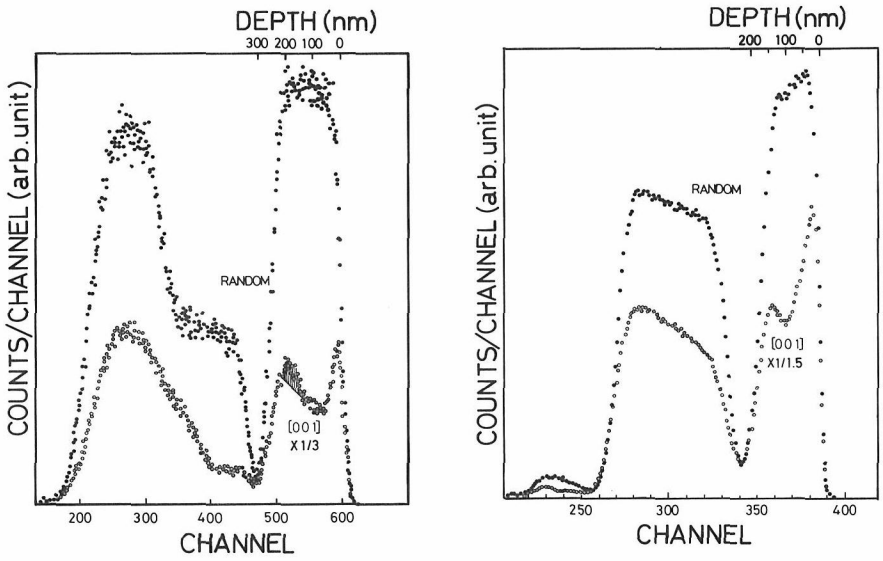

Fig. 8 [001] aligned and random energy spectra of He ions backscattered from (a) PbTe/SnTe and (b) PbS/SnTe. The peak at the lower energy tail of the ions scattered from Pb atoms in the [001] aligned spectrum from PbTe/SnTe, which is indicated by shaded lines, is due to the direct scattering of channelling ioons from misfit dislocations. No such peak is seen in the spectrum from PbS/SnTe.

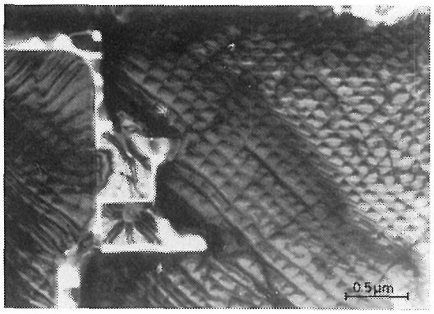

Fig. 9 An electron micrograph of PbTe/SnTe bicrystal, where the substrate SnTe has island structure. Misfit dislocations are observed only at large SnTe islands. Double crosses on smaller islands are extinction contours caused by spherical bending of the island crystals.

than about 10 nm. Misfit dislocations are observed mainly on the larger SnTe islands, while the smaller islands are heavily strained to show extinction contours characteristic to the spherically deformed crystal. Since the dislocated bicrystals do not show such bending, this micrograph demonstrates that the misfit of two crystals is relieved by the introduction of misfit dislocations on the interface. The misfit strain is smaller at smaller substrate crystal and is relieved by the elastic bending of the bicrystal, while the larger strain in larger bicrystal is relieved by the introduction of dislocations. It is expected that this bending of small bicrystals occurs in other bicrystal system studeid here. Analysis of the crystal strain on the size of the bicrystal and on the introduction of misfit dislocations are now in progress.

ACKNOWLEDGEMENT

We are grateful to the members of the Department of Nuclear Engineering for the use of the 4 MV Van de Graaff accelerator. Our thank extends to our collaborators, Dr. A. Kyoshima, Mrs. S. Sawada, Y. Kawagoe, H. Kawauchi and M. Suzuki. This work was partly supported by Grant-in-Aid for Scientific Research on Priority Areas "Crystal Growth Mechanism in Atomic Scale".

REFERENCES

(1) A. G. Mikolaichuk and D. M. Freik, *Sov. Phys.-Solid State,* **11**, 2033 (1970).
(2) L. S. Palatnik, L. P. Zozuya and V. M. Kosevich, *Sov. Phys.-Solid State,* **11**, 1460 (1970).
(3) J. W. Mathews, in "*Dislocations in Solids*" vol. 2, ed. F, R, N, Nabarro (North-Holland, Amsterdam, 1979) p.461.
(4) G. Honjo and K. Yagi, in "*Current Topics in Materails Science*" vol. 6, ed. E. Kaldis (North-Holland, Amsterdam, 1980) p.195.
(5) For instance, K. Kimura, M. Hasegawa, Y. Fujii, M. Suzuki, Y. Susuki and M. Mannami, *Nucl. Instrum. & Meth.,* **B33**, 358 (1988).
(6) Y. Kawagoe, Master Thesis, Kyoto University 1984.
(7) H. Kawauchi, Master Thesis, Kyoto University 1986.
(8) M. Suzuki, H. Kawauchi, K. Kimura and M. Mannami, *Surf. Sci.,* **204**, 223 (1988).
(9) J. D. Eshelby, in "*Dislocations in Solids*" vol 1, ed. F, R, N, Nabarro (North-Holland, Amsterdam, 1979) p. 167.
(10) Y. Fujii, S. Fujiwara, K. Kimura and M. Mannami, Radiat. Effects and Defects in Solids, *in press.*
(11) M. Tsuji, Y. Mizuno, Y. Susuki and M. Mannami, *J. Cryst. Growth* **108**, 817 (1991).
(12) S. Sawada, K. Kimura and M. Mannamim, *Jpn. J. Appl, Phys.,* **22**, 1464 (1983).